# Exceptional Solvent Tolerance in *Yarrowia lipolytica* Is Enhanced by Sterols

Caleb Walker, Seunghyun Ryu, Cong T. Trinh*

Department of Chemical and Biomolecular Engineering, University of Tennessee, TN 37996

*Corresponding author. Email: ctrinh@utk.edu. Tel: 865-974-8121

## Abstract

Microbial biocatalysis in organic solvents such as ionic liquids (ILs) is attractive for making fuels and chemicals from complex substrates including lignocellulosic biomass. However, low IL concentrations of 0.5−1.0 % (v/v) can drastically inhibit microbial activity. In this study, we engineered an exceptionally robust oleaginous yeast *Yarrowia lipolytica*, YlCW001, by adaptive laboratory evolution (ALE). The mutant YlWC001 shows robust growth in up to 18% (v/v) 1-ethyl-3-methylimidazolium acetate ([EMIM][OAc]), which makes it the most IL-tolerant microorganism published to our knowledge. Remarkably, YlCW001 exhibits broad tolerance in most commonly used hydrophilic ILs beyond [EMIM][OAc]. Scanning electron microscopy revealed that ILs significantly damage cell wall and/or membrane of wildtype *Y. lipolytica* with observed cavities, dents, and wrinkles while YlCW001 maintains healthy morphology even in high concentrations of ILs up to 18% (v/v). By performing comprehensive metabolomics, lipidomics, and transcriptomics to elucidate this unique phenotype, we discovered that both wildtype *Y. lipolytica* and YlCW001 reconfigured membrane composition (e.g., glycerophospholipids and sterols) and cell wall structure (e.g., chitin) under IL-stressful environments. By probing the steroid pathway at transcriptomic, enzymatic, and metabolic levels, we validated that sterols (i.e., ergosterol) are a key component of the cell membrane that enables *Y. lipolytica* to resist IL-responsive membrane damage and hence tolerate high IL concentrations. This study provides a better understanding of exceptional robustness of *Y. lipolytica* that can be potentially harnessed as a microbial manufacturing platform for production of fuels and chemicals in organic solvents.


**Keywords:** *Yarrowia lipolytica*; ionic liquid; adaptive laboratory evolution; stress responsive metabolism; lipidomics; metabolomics; glycerophospholipids; sterols

## Significance

Robustness is an important production phenotype for any industrial microbial catalyst to acquire but it is complex and difficult to engineer. Through adaptive laboratory evolution, in combination with comprehensive omics analysis, we shed light on the underlying mechanism of how *Y. lipolytica* restructures its membrane to tolerate high levels (up to 18% v/v) of ILs, which makes our evolved strain the most IL-tolerant microorganism reported to date. Specifically, we discovered that sterols play a key role for enhancing exceptional IL tolerance in *Y. lipolytica*. Overall, this study provides fundamental understanding and engineering strategy for exceptional robustness of oleaginous yeasts to improve growth and novel biotransformation in inhibitory organic solvents.

# Introduction

Robustness is an important phenotype for any industrial microbe to acquire for biosynthesis of desirable molecules (1-3). Recently, microbial biocatalysis in green organic solvents such as ionic liquids (ILs) has become attractive to produce biofuels (4, 5) and high-value bioproducts (6-8). One key advantage is that ILs can effectively process complex and recalcitrant substrates such as lignocellulosic biomass for microbial fermentation (9-13). Further, these ILs can function as extractants for *in situ* separation of desirable molecules (14-18). Thus, it is highly desirable to harness novel microbes for biocatalysis in organic solvents.

To perform novel biotransformation in ILs, microbes need to be robust to tolerate high concentrations of solvents (19, 20). These solvents are inhibitory because they severely disrupt cell membranes and intracellular processes (21-23). For applications such as simultaneous saccharification and fermentation of IL-pretreated lignocellulosic biomass, microbes that are active in high IL-containing media are desirable because expensive IL washing and recycling steps prior to fermentation are not needed (7, 24). Unfortunately, most industrially-relevant platform organisms, *Escherichia coli* and *Saccharomyces cerevisiae*, are severely inhibited in IL-containing media even at low concentrations, for instance, 1% (v/v) [EMIM][OAc] (25, 26).

To overcome IL toxicity, various targeted and evolutionary engineering strategies have been performed. For instance, an *E. coli* strain was engineered to produce desirable chemicals from IL-pretreated biomass in the presence of 100 mM (< 2% v/v) [EMIM][OAc] by mutating the endogenous transcriptional regulator RcdA (P7Q) to de-repress expression of the inner membrane pump YbjJ (27) or overexpressing a heterologous IL-specific efflux pump, EliA, isolated from *Enterobacter lignolyticus* (28, 29). Likewise, adaptive laboratory evolution (ALE) was conducted to generate an *E. coli* mutant with robust growth in 500 mM (8.3 % (v/v)) [EMIM][OAc] (30). By

deleting a highly IL-responsive, mitochondrial serine/threonine kinase gene *ptk2* (which activates a plasma-membrane proton efflux pump Pma1), an engineered *S. cerevisiae* strain became capable of tolerating > 2% (v/v) [EMIM][Cl] (31). Even though the above engineering strategies resulted in enhanced IL-tolerant phenotypes, the engineered strains are not tolerant enough to robustly grow in in 10 % (v/v) ILs unlike *Y. lipolytica*. This highlights the complexity of IL-tolerant phenotypes and the limited understanding of IL-tolerant mechanisms.

Synergistically, exploring microbial and genetic diversity can potentially discover novel genotypes conferring novel IL tolerance that typically does not exist in the current platform organisms. Bioprospecting the tropical rainforest soil resulted in isolation of a novel *Enterobacter lignolyticus* that could survive in 0.5 M (6.6 % (v/v)) [EMIM][Cl] (29). Likewise, screening microbial diversity from a collection of 168 fungal yeasts identified 13 robust strains that can tolerate up to 5% (v/v) [EMIM][OAc], including *Clavispora*, *Debaryomyces*, *Galactomyces*, *Hyphopichia*, *Kazachstania*, *Meyerozyma*, *Naumovozyma*, *Wickerhamomyces*, *Yarrowia*, and *Zygoascus* genera (20). Among the non-conventional yeasts, *Y. lipolytica* is attractive for fundamental study and industrial application due to its oleaginous nature (32, 33) and robustness in extreme environments (20, 34-36). Remarkably, wildtype *Y. lipolytica* (ATCC MYA-2613) exhibited robust growth in media containing at least 10% (v/v) [EMIM][OAc] while producing 92% maximum theoretical yield of alpha-ketoglutarate from IL-pretreated cellulose (7). Currently, mechanisms of IL toxicity and superior tolerance in microorganisms are not completely elucidated (37). For instance, since prokaryotes and eukaryotes have different membrane structures, it is unclear of how their membranes are reconfigured to resist IL interference.

Given the endogenous robustness of *Y. lipolytica*, the goal of this study is to illuminate the underlying mechanisms for IL toxicity and exceptional tolerance of the wildtype strain and evolved

mutant generated by ALE. Particularly, we aim to elucidate how *Y. lipolytica* restructures its membrane to resist IL disruption and modulates sterol levels to improve exceptional IL tolerance.

## Results

### Generate robust *Y. lipolytica* mutants via ALE as a basis for elucidating IL-tolerant mechanism

***Y. lipolytica has a novel endogenous metabolism conferring exceptional IL tolerance.*** Since wildtype *Y. lipolytica* can grow in at least 10% (v/v) [EMIM][OAc] (7), we hypothesize that it has a novel endogenous metabolism conferring exceptional IL robustness. To test this, we performed ALE to generate *Y. lipolytica* mutants with enhanced tolerance to high concentrations of the benchmark IL, [EMIM][OAc] (Fig. 1, Step1). First, wildtype *Y. lipolytica* was grown in a medium containing 5% (v/v) [EMIM][OAc] and transferred into a medium containing progressively increased concentrations of [EMIM][OAc], 8% and 10% (v/v). Remarkably, *Y. lipolytica* was able to grow in 5%, 8%, and 10% (v/v) [EMIM][OAc] with specific growth rates of 0.063 ± 0.005 1/h, 0.056 ± 0.033 1/h and 0.060 ± 0.004 1/h, respectively, without any significant growth inhibition (Fig. 2A). When *Y. lipolytica* was transferred into a medium containing 12% (v/v) [EMIM][OAc], it initially exhibited growth inhibition with significantly reduced specific growth rate of 0.034 ± 0.001 1/h. However, after 16 generations in 12% (v/v) [EMIM][OAc], the specific growth rate was improved up to 0.080 ± 0.006 1/h and maintained for another 22 generations. Next, we increased the concentration of [EMIM][OAc] to 15% (v/v) and continued ALE. The first transfer from 12% (v/v) to 15% (v/v) reduced the specific growth rate by ~62% but cells recovered within 5 generations (0.078 ± 0.014 1/h) and the growth was maintained for an additional 23 generations. We further increased the concentration of [EMIM][OAc] to 18% (v/v)

and continued serial transfers for another 106 generations. At the end of ALE (200 generations), we isolated the top performing *Y. lipolytica* mutant, YlCW001, growing in up to 18% (v/v) [EMIM][OAc] with a specific growth rate of 0.055 ± 0.006 1/h (Fig. 1, Step 2).

***Exceptional IL-tolerant phenotype of the evolved mutant YlCW001 is stable***. To use YlCW001 for downstream characterization, we subjected it to irreversibility and stability tests (Fig. 1, Step 3). For irreversibility test, three biological replicates of wildtype and YlCW001 strains were grown in medium containing 8% (v/v) [EMIM][OAc] to lessen abrupt osmotic shock driven by IL. Mid-exponentially growing cells were then transferred into the medium containing glucose and 18% (v/v) [EMIM][OAc], and the cell growth was investigated. While growth of wildtype *Y. lipolytica* was completely inhibited, YlCW001 was able to grow with a specific growth rate of 0.059 ± 0.001 1/h (Fig. 2B), comparable to that measured from ALE in 18% (v/v) [EMIM][OAc]. These results confirmed that the improved IL-tolerance for YlCW001 is irreversible.

Further, we investigated stability of YlCW001 by reviving the frozen glycerol stock in the liquid medium containing glucose and [EMIM][OAc] (Fig. 1, Step 3). Like the irreversibility test, we tested cell growth of three biological replicates of YlCW001 in 18% (v/v) [EMIM][OAc] using glucose as a carbon source. The measured specific growth rate was similar to that from ALE and the irreversibility test (data not shown), proving that YlCW001 is a stable strain.

***YlCW001 exhibits broad tolerance to a wide range of hydrophilic ILs.*** To test whether the IL-evolved strain YlCW001 exhibits broad IL-tolerant phenotypes, we investigated the following hydrophilic ILs: 1-ethyl-3-methylimidazolium acetate ([EMIM][OAc]), 1-ethyl-3-methylimidazolium chloride ([EMIM][Cl]), 1-ethyl-3-methylimidazolium bromide ([EMIM][Br]), 1-allyl-3-methylimidazolium chloride ([AMIM][Cl]), 1-butyl-3-

methylimidazolium acetate ([BMIM][OAc]), 1-butyl-3-methylimidazolium chloride ([BMIM][Cl])), and 1-butyl-3-methylimidazolium bromide ([BMIM][Br]). We selected these ILs for testing because they can effectively solubilize various types of recalcitrant lignocellulosic biomass and are known to be very inhibitory to microbial growth (38, 39). Since wildtype growth was inhibited in 10% (v/v) and lethal in 18% (v/v) [EMIM][OAc] (Fig. 2C), we characterized these strains in two different concentrations of ILs, 0.6 M and 1.09 M (equivalent to 10% and 18% (v/v) of [EMIM][OAc], respectively).

Growth characterization in 0.6 M ILs shows that YlCW001 outperformed wildtype *Y. lipolytica* for all ILs except [EMIM][Cl], for which similar specific growth rates were observed (Fig. 2D). Remarkably, YlCW001 growth was not affected by all tested ILs regardless of imidazolium alkyl chain length and conjoined anion, excluding [BMIM][OAc], which at 0.6 M was lethal to both wildtype and YlCW001 (Fig. 2D). In 1.09 M ILs, wildtype *Y. lipolytica* exhibited substantial growth inhibition in [EMIM][Cl] and [EMIM][Br] and no growth in [AMIM][Cl], [BMIM][Cl], [EMIM][OAc], [BMIM][Br], and [BMIM][OAc] (Fig. 2E). Strikingly, the evolved strain YlCW001 displayed robustness in all ILs except [BMIM][OAc] confirming broad tolerance to ILs (Fig. 2E).

Inhibition of YlCW001 growth was detected in the following order: [BMIM][OAc] $\gg$ [BMIM][Br] $\approx$ [BMIM][Cl] $\approx$ [EMIM][OAc] $>$ [AMIM][Cl] $>$ [EMIM][Br] $\approx$ [EMIM][Cl]. While 0.6 M [BMIM][OAc] entirely inactivated growth of both wildtype and YlCW001, the mutant tolerated 0.3 M [BMIM][OAc] with a specific growth rate of 0.07 $\pm$ 0.02 1/h which remained lethal to wildtype (SI Appendix, Fig. S1).

Overall, we demonstrated that *Y. lipolytica* possesses novel endogenous metabolism conferring high IL tolerance by generating a novel, exceptionally robust *Y. lipolytica* mutant via

ALE. The evolved strain YlCW001 is stable and exhibits broad tolerance towards the hydrophilic ILs in this study. This significant result provides a strong basis for elucidating the underlying mechanism of solvent toxicity in *Y. lipolytica*.

**Elucidate IL-responsive physiology and metabolism in *Y. lipolytica* strains**

***Cell membrane and morphology of the evolved mutant resist IL interference.*** Since ILs are known to disrupt the cell membrane (40-42), we hypothesize that the mutant YlCW001 might have adapted its membrane structure to cope with inhibitory ILs. To test this, we used scanning electron microscopy (SEM) to examine cell membranes and morphologies of both the wildtype and mutant responsive to 0% and 18% (v/v) [EMIM][OAc], 0.3M [BMIM][OAc], and 0.6M [BMIM][OAc].

As a positive control, we observed healthy morphologies for both the wildtype and mutant in no-IL media (Fig. 3A, 3B). However, when exposed to 18% (v/v) [EMIM][OAc], the wildtype developed cavities, dents, and wrinkles along the cell surface, clearly demonstrating that cell membrane and/or cell wall components were severely damaged by the IL (Fig. 3C). This phenotype is consistent with the complete growth inhibition of the wildtype observed at this high IL concentration (Fig. 2B, 2C). In contrast, the evolved strain YlCW001 displayed barely any signs of membrane damage in 18% (v/v) [EMIM][OAc] (Fig. 3D).

Likewise, when being exposed to a more toxic IL, [BMIM][OAc], the wildtype exhibited significant morphology deconstruction in both 0.3M and 0.6M [BMIM][OAc] (Fig. 3E, 3G). Strikingly, YlCW001 displayed no significant morphological defects (Fig. 3F, 3H) although growth was marginally inhibited in 0.3M and lethal in 0.6M [BMIM][OAc] (SI Appendix, Fig. S1 and Fig. 2D).

178 ***Intracellular metabolism of Y. lipolytica is perturbed in response to IL exposure.*** To
179 demonstrate that intracellular metabolism of *Y. lipolytica* is also perturbed in IL, we performed
180 untargeted metabolomics and lipidomics for both the wildtype and YlCW001 growing in media
181 containing 0% and 8% (v/v) [EMIM][OAc]. Our results identified a total of 37 and 40 significantly
182 perturbed pathways in wildtype and YlCW001, respectively, growing in 8% (v/v) [EMIM][OAc]
183 as compared to the wildtype growing in no IL (Fig. 3I and SI Appendix, Table S1). Among these
184 pathways, 29 were found perturbed in both wildtype and YlCW001. These pathways are mostly
185 comprised of amino acid synthesis/degradation, nucleosides and nucleotides
186 synthesis/degradation, but also contain vitamins synthesis (coenzyme A, thiamine, folate, and
187 biotin biosynthesis etc.), carbohydrates biosynthesis/degradation (GDP-mannose biosynthesis,
188 gluconeogenesis, galactose degradation, etc.), respiration (TCA cycle, glyoxylate cycle, etc.),
189 sterols biosynthesis, and some of the central metabolic pathways responsible for generating
190 precursor metabolites and energy (glycolysis, pentose phosphate pathway, etc.).

191 Furthermore, we found that YlCW001 had a total of 19 perturbed metabolic processes in
192 media without IL in comparison to the wildtype without IL (Fig. 3I and SI Appendix, Table S1).
193 Notably, 15 of these pathways were also perturbed in YlCW001 and wildtype growing in 8% (v/v)
194 [EMIM][OAc] mostly enriched for amino acid biosynthesis/degradation but also included sterol
195 biosynthesis. Overall, we identified significant perturbation of intracellular metabolism for both
196 strains subjected to IL. While the bulk of these pathways are enriched for central carbon
197 metabolism, our untargeted metabolomics and lipidomics identified sterols biosynthesis as the
198 only lipid pathway significantly perturbed among all three biological conditions (wildtype 8%,
199 YlCW001 8%, YlCW001 0%) in comparison to the wildtype without IL (Fig. 3I).
200

***Remodeling of cell membrane enhanced IL-tolerance in Y. lipolytica.*** The outer-surface of the eukaryotic yeast is a multifaceted, permeable barrier composed of a plasma membrane (i.e., glycerophospholipids, sterols, sphingolipids) and cell wall (i.e., chitin, glucan, mannoproteins) that together, allow the cell to adapt to a variety of environmental conditions to maintain cellular homeostasis (43-46). Based on SEM images, untargeted metabolomics, and potential mechanisms of IL-toxicity (21, 47-50), we hypothesized that remodeling of cellular membrane and/or cell wall is one key IL stress-responsive process in *Y. lipolytica*. We aimed to identify critical membrane and cell wall components conferring exceptional IL-tolerance of both wildtype and YlCW001 strains by investigating IL-responsive glycerophospholipid, fatty acid, sterol, and chitin metabolism in benchmark IL, [EMIM][OAc].

***Y. lipolytica reduced chitin in the presence of ILs***. Chitin is one of the most insoluble biopolymers, even for ILs (47, 51). In *S. cerevisiae*, it has been reported that metabolism of chitin, a cell wall component known to influence membrane rigidity and elasticity, is increased upon cell wall integrity stresses (52). Since *Y. lipolytica* contains a relatively high content of chitin relative to other yeasts (e.g., ~10-15% *Y. lipolytica*; ~1-3% *S. cerevisiae*), we investigated how its membrane chitin is responsive to IL exposure. Counter-intuitively, we observed a ~2-fold reduction in chitin content for both strains upon IL-exposure (SI Appendix, Fig. S2). Of note, we were unable to detect any statistically significant differences in chitin levels between the wildtype and YlCW001 strains as they behaved similarly in 0% and 8% [EMIM][OAc]. While chitin may contribute to native *Y. lipolytica* IL-robustness, our results suggest chitin is not responsible for the enhanced IL-tolerance of YlCW001.

***Y. lipolytica modulated glycerophospholipid composition in the presence of ILs.*** Upon IL exposure, the backbone and headgroups of the *glycerophospholipids* are expected to interact with

both cations and anions of ILs. To understand IL toxicity and tolerance, we next investigated IL-responsive glycerophospholipid metabolism by performing targeted lipidomics on individual headgroup species (i.e., phosphatidylcholine, PC; phosphatidylinositol, PI; phosphatidic acid, PA; phosphatidyl glycerol, PG; phosphatidylserine, PS; phosphatidylethanolamine, PE; and cardiolipins, CL) for both strains in 0% and 8% (v/v) [EMIM][OAc]. In no IL media, we found that YlCW001 contained a larger amount of each glycerophospholipid species than the wildtype (Fig. 4 A-G). In 8% (v/v) [EMIM][OAc], most components of glycerophospholipids, including PC, PI, PA, PG, and CL, were upregulated in both strains, except that PE and PS exhibited different trends. The PE content of both strains remained unchanged (relative to wildtype 0%) while the PS content increased (Fig. 4E, 4F). Additionally, the mutant in media without IL contained statistically greater basal amounts of PE and PS species ($p \leq 0.01$) than the wildtype.

Overall, we found IL-responsive, upregulated glycerophospholipid production of all headgroup species except PE. Interestingly, we also observed greater basal glycerophospholipid content in YlCW001 over the wildtype in 0% IL. These findings of membrane restructuring likely contribute to IL-toxicity resistance in *Y. lipolytica.*

***ILs modulated the fatty acid composition of Y. lipolytica.*** Since fatty acids can modulate membrane fluidity (53, 54), we next analyzed the effect of ILs on the fatty acid profiles of wildtype and YlCW001 strains. The most striking differences were observed for C16:1 and C18:1 fatty acid moieties (Fig. 4H). We found that both strains exposed to IL induced production of C16:1 (7 mol%, $p < 0.01$) fatty acids unlike the wildtype strain without IL, which produced none. In contrast, the wildtype without IL contained mostly C18:1 fatty acids (49 mol%) while all other biological conditions shifted to the di-unsaturated C18:2 moiety (29-36 mol%, $p < 0.02$). Interestingly, YlCW001 in media without IL behaved similarly to IL-exposed strains, with

247 significant increases in C16 and C18:2 production. We did not observe a statistically significant
248 difference between total saturated and unsaturated fatty acid moieties in both conditions. Taken
249 together, IL-exposed cells (and YlCW001 0%) produced C16:1 fatty acids (non-existent in
250 wildtype 0%) with statistically significant larger ratios of C16:C18 and (C18:2):(C18:1) moieties
251 in comparison to the wildtype without IL. Shorter chain lengths with higher degrees of
252 unsaturation in fatty acid moieties of the cell membrane are likely expected to increase membrane
253 fluidity (46). These results indicate that fatty acid metabolism is IL-modulated in *Y. lipolytica* and
254 altered in YlCW001, even without IL.

255 ***YlCW001 increased sterols in the presence of ILs***. We next investigated the functional
256 role of sterols for IL tolerance in *Y. lipolytica* because i) the sterol biosynthesis pathway was
257 perturbed in untargeted omics analysis, ii) sterols (e.g., cholesterol) can impede cation-insertion
258 into the membrane (48), and iii) sterols greatly influence membrane fluidity (55, 56). In IL, we
259 observed ~2 fold increase ($p$ = 0.013) in ergosterol content of YlCW001 over the wildtype strain
260 (Fig. 5D). Counter-intuitively, we found the largest ergosterol concentrations in both strains
261 without IL. We were unable to identify any other sterol pathway intermediates (e.g., squalene,
262 lanosterol, etc.), in agreement with literature concluding ergosterol as the dominant sterol in yeast
263 (57). These results imply that IL affects sterol biosynthesis, and unlike the wildtype, YlCW001
264 adapted by enhancing membrane sterols in response to IL exposure.

265 **Sterol biosynthesis is one key IL-responsive process to improve IL-tolerance *in Y. lipolytica***
266 We hypothesized that ergosterol content is a critical component of the membrane contributing to
267 the enhanced IL-tolerance of YlCW001 since we observed a greater ergosterol content in
268 YlCW001 than the wildtype upon exposure to IL (Fig. 5D). To validate the key role of sterols, we

investigated genetic and enzymatic details of how *Y. lipolytica* modulates the sterol pathway in response to IL.

We first characterized the mRNA expression levels of 14 genes in the steroid biosynthesis pathway of mid-exponentially growing wildtype and YlCW001 cells cultured in 0% and 8% [EMIM][OAc] (Fig. 5A). We found that 10 of the 14 steroid pathway genes were upregulated > 2 fold in IL-exposed YlCW001 as compared to the wildtype in 0% IL (Fig. 5B). Significantly, six of these genes, including Ster5 (YALI0B23298g), Ster6 (YALI0F11297g), Ster8 (YALI0B17644g), Ster10-1 (YALI0E32065g), Ster10-2 (YALI0B17204g), and Ster11 (YALI0D20878g), were upregulated > 4 fold in IL-exposed YlCW001 over the wildtype in 0% IL. As for the wildtype in 8% IL, we found only 1 of the 14 steroid pathway genes, Ster10-2 (YALI0B17204g), significantly upregulated against the wildtype without IL. Without IL, the steroid genes in YlCW001 were relatively constant or marginally downregulated in comparison to the wildtype.

To confirm the contribution of sterols in IL-tolerance at the enzymatic level, we next treated the wildtype and YlCW001 strains with fluconazole, a commonly used anti-fungal drug that inhibits cytochrome P450 enzyme 14α-demethylase (Ster4, Fig. 5A) critical for sterol biosynthesis (58). We characterized growth of the wildtype and YlCW001 in media containing either 0% or 8% (v/v) [EMIM][OAc] with incremental concentrations of fluconazole (Fig. 5C). We expected that fluconazole inhibits sterol biosynthesis and hence incurs the adverse effect of IL-tolerance, specifically to a greater extent in the wildtype than in YlCW001. In media containing no IL, we found that fluconazole inhibited growth for both the wildtype and YlCW001 ($IC_{50}$ = 25 μg/mL), (Fig. 5C). In the presence of 8% (v/v) [EMIM][OAc], inhibition of fluconazole became more significant. Remarkably, YlCW001 could tolerate up to 25 μg/mL fluconazole while this

292 concentration proved lethal for the wildtype (Fig. 5C). Taken together, the mutant in IL increased
293 gene expression, better tolerated enzymatic inhibition of the steroid biosynthesis pathway, and
294 elevated the end-product (i.e., ergosterol) biosynthesis in comparison to the wildtype.
295

296 ## Discussion

297 Microbial biocatalysis in ILs is novel for biosynthesis of fuels and chemicals. For instance,
298 the imidazolium-based ILs (e.g., [EMIM][OAc]) are effective for reducing lignocellulosic biomass
299 recalcitrance (59) to be used for downstream fermentation but greatly inhibit microbial growth
300 even at low concentrations (47, 60). This incompatibility presents a significant barrier for novel
301 microbial biocatalysis in ILs. While mechanisms of IL-toxicity have been proposed (22, 29, 31),
302 the complete picture is unclear of how cells resist to ILs and whether these cells can adapt to
303 achieve IL-tolerance for industrial compatibility (19, 20, 27). To illuminate the mechanisms of IL
304 toxicity and enhanced tolerance (Fig. 6), we characterized naturally IL-tolerant *Y. lipolytica* and
305 its superior evolved mutant, YlCW001, generated by ALE (Fig. 2A).

306 Imidazolium-based ILs inhibit the cell by inserting their alkyl chains into the hydrophobic
307 core of the plasma membrane (Fig. 6B, 6E, 6C, and 6F) (41, 48). ILs with longer alkyl chains
308 become more lipophilic (21, 61) and cause greater disruption of the membrane as supported by
309 growth rates in various ILs ([BMIM] ≫ [AMIM] ~ [EMIM]) (Fig. 2D, 2E). The conjoint anion
310 likely re-associates with the cation imbedded into the membrane causing greater membrane
311 disturbance (48). The tendency of an anion to interact with the cation intensifies with increasing
312 basicity, which increases IL toxicity as demonstrated by reduced growth rates in various ILs
313 ([OAc] ≫ [Br] ~ [Cl]) (Fig. 2D, 2E).

Consequences of IL membrane disruption increase membrane fluidity (e.g., ionic surfactant) (23, 49) and impose lateral pressure on the membrane (50, 62) as evidenced by cavities, dents, and wrinkles in SEM images (Fig. 3C, 3E, 3G) and dramatic remodeling of lipids in *Y. lipolytica* (Fig. 4). In addition, harmful interactions between the IL and membrane result in a cascade of detrimental effects on cellular processes including DNA damage, enzyme inactivation, and protein degeneration (59, 63-65), as observed by reduced sterol and chitin contents (Fig. 5D and SI Appendix, Fig. S2) and perturbation of intracellular metabolism (Fig. 3I) of IL-exposed wildtype and YlCW001 strains.

Wildtype and YlCW001 strains combatted IL toxicity in part by rewiring membrane compositions to reduce membrane permeability and bilayer buckling pressure (imposed by ILs) (66, 67). Both strains overproduced all glycerophospholipid species except PE (Fig. 4F), which is vulnerable to lateral pressure (68, 69). In contrast to the wildtype, YlCW001 is more robust because it adapts to produce more sterols, e.g., ergosterol upon IL-exposure (Fig. 5D), that function to maintain membrane fluidity and stability (55). This novel phenotype is evidenced by a significant upregulation of sterol biosynthesis genes (Fig. 5B) and improved enzymatic-tolerance to steroid-inhibiting drug, fluconazole (Fig. 5C) (58, 70). The result is also consistent with molecular simulations demonstrating sterols impede IL cations from inserting into artificial membranes (71-73).

Taken together, ILs inhibit cell growth by fluidizing the membrane and inflicting lateral pressures that destroy cellular homeostasis (Fig. 6B, 6C). Our research provides strong evidence of how intracellular processes of *Y. lipolytica* are rewired to remodel cell membranes upon IL-exposure. Comprehensive metabolic, transcriptomic, and enzymatic analyses provide strong evidence that sterols (i.e., ergosterol) are critical membrane components conferring IL-tolerance

in *Y. lipolytica* and enhanced IL-robustness in YlCW001, functioning to impede cation insertion and maintain membrane homeostasis (72) (Fig. 6E, 6F). Although in this study we focused on elucidating IL-responsive metabolism specific to lipid membrane remodeling, future work will aim to determine the evolved genotype of YlCW001 to further understand IL-tolerance in *Y. lipolytica* towards the application of reverse engineering IL-robustness in diverse, industrially-relevant microorganisms.

## Materials and Methods

### Strains

*Yarrowia lipolytica* (ATCC MYA-2613), a thiamine, leucine, and uracil auxotroph, was purchased from American Type Culture Collection. The evolved strain YlCW001 was isolated after 200 generations in gradually increased concentrations of [EMIM][OAc] up to 18% (v/v).

### Medium and culturing conditions

*Growth medium.* ALE, irreversibility testing, and broad IL tolerance studies were conducted in defined media containing 6.7 g/L of yeast nitrogen base without amino acids (cat# Y0626, Sigma-Aldrich, MO, USA), 10 g/L of glucose, 100 mg/L of ampicillin, 50 mg/L of kanamycin, 30 mg/L of chloramphenicol, and various concentrations of ILs. Leucine (cat# 172130250, Acros Organics, CA, USA) and uracil (cat# 157301000, Acros Organics, CA, USA) were added to the media at concentrations of 190 mg/L and 20 mg/L, respectively.

For all other growth studies, 380 mg/L of leucine and 76 mg/L uracil were used. All ILs, including 1-ethyl-3-methylimidazolium acetate [EMIM][OAc] (>95 % purity), 1-ethyl-3-methylimidazolium chloride [EMIM][Cl] (>98% purity), 1-ethyl-3-methylimidazolium bromide [EMIM][Br] (99% purity), 1-allyl-3-methylimidazolium chloride [AMIM][Cl] (>98% purity), 1-

butyl-3-methylimidazolium acetate [BMIM][OAc] (>98% purity), 1-butyl-3-methylimidazolium chloride [BMIM][Cl] (99% purity), and 1-butyl-3-methylimidazolium bromide [BMIM][Br] (99% purity), were purchased from the Ionic Liquids Technologies Inc. (IoLiTec, AL, USA). Unless specifically mentioned, all experiments were performed with biological triplicates.

*Adaptive laboratory evolution.* ALE experiment was performed by serial dilution of *Y. lipolytica* in sequentially increasing concentrations of [EMIM][OAc] in 6-well plates with 3 mL working volume using an incubating microplate shaker (cat# 02-217-757, Fisher Scientific, PA, USA) at 28°C and 350 rpm with adhesive, breathable seals to prevent cross contamination (cat# 50-550-304, Fisher Scientific, PA, USA). For each serial dilution, the top performing triplicate was transferred during mid-exponential growth phase into fresh medium at an initial optical density (OD) at 600 nm of 0.2. Increasing concentrations of [EMIM][OAc] were selected to achieve a specific growth rate $\geq 0.02$ 1/h. The maximum specific growth rates of all three technical replicates were calculated for each serial dilution using a minimum of three time points per replicate. After 200 generations of ALE, the top performing replicate culture was spread onto a petri plate containing defined medium with 10 g/L glucose and 20 g/L agar. The plate was incubated at 28$^{o}$C for 36-48 hours. Single colonies were isolated and individually streaked onto fresh petri plates. This process was repeated once more to ensure isolation of purified colonies. Purified colonies (from three iterations of plate dilutions) were individually tested in the same growth conditions and [EMIM][OAc] concentration at which the evolved strain was originally collected to determine irreversibility. Individual cultures (from purified colonies) were collected and stored in glycerol at -80°C before streaking onto fresh petri plates, repeating three plate isolations, and retesting the irreversibility of the purified colonies to determine stability of YlCW001.

## Analytical methods

*Metabolomics.* Three biological replicates of the wildtype and YlCW001 were grown in media containing 0% or 8% (v/v) [EMIM][OAc] and collected at the late-exponential growth phase for metabolomics analysis. Samples were immediately quenched in liquid nitrogen and stored at -80°C prior to extraction. Metabolites were extracted from a minimum of 1 $x10^7$ cells in 400µL of the extraction solvent by incubating at -20°C for 20 min (74). The extraction solvent consists of 40:40:20 methanol:acetonitrile:water containing 0.1M formic acid. The soluble fraction was separated by centrifugation at 13,700 x g, 4°C for 5 minutes. To ensure complete extraction of cellular metabolites, we repeated extraction 3 times per sample. A total of 1.2 mL of solvent-soluble metabolite samples were subjected to drying under a stream of nitrogen at 4°C overnight to evaporate solvent. Lyophilized metabolites were reconstituted in 300µL of sterile water and analyzed by liquid chromatography mass spectrometer (LC-MS).

Metabolites were analyzed with an Exactive Plus orbitrap mass spectrometer (Thermo Scientific, San Jose, CA) equipped with Synergi 2.5µm Hydro-RP 100 (100 x 2.00 mm, Phenomenex, Torrance, CA, USA) set to 25°C. The LC-MS method analyzed in full scan negative ionization mode with an electrospray ionization source as previously described (75).

*Lipidomics.* Late-exponentially growing wildtype and YlCW001 cells cultured in 0% and 8% (v/v) [EMIM][OAc] were used for lipidomics study. Samples were immediately quenched in liquid nitrogen and stored at -80°C. After thawing on ice, samples were centrifuged for 3 minutes at max speed, 4°C before removing supernatant. Next, cell pellets were re-suspended in 800uL of 0.1N hydrochloric acid:methanol 1:1 with 400uL of chloroform and disrupted with glass beads using a mini bead beater for 5 minute intervals until > 95% of cells were visually disrupted. Disrupted cells were vortexed and centrifuged at 4°C for 5 minutes before extracting the organic

406 phase into glass vials. Finally, samples were dried under a stream of nitrogen overnight at 4°C
407 and reconstituted in 300uL of 9:1 methanol:chloroform before transferring into auto-sampler vials.
408 Lipid extracts were analyzed in positive and negative ionization modes with an Exactive Plus
409 orbitrap mass spectrometer (Thermo Fisher Scientific, San Jose, CA) equipped with an
410 electrospray ionization probe and a Kinetex HILIC column (150 mm x 2.1 mm, 2.5 µm)
411 (Phenomenex, Torrance, CA, USA) as previously described (76) except that lipid features were
412 verified with external standards instead of fragments.

413 *Untargeted LCMS analysis.* Metabolomics and lipidomics raw files created by Xcalibur
414 were imported into XCMS online and analyzed in pairwise jobs against the control data set,
415 wildtype in 0% IL (77). XCMS resulting metabolic features were exported and features with
416 intensity fold changes < 2 were removed. These pairwise sets of 'perturbed' metabolic features
417 were analyzed with metaboanalyst (78) using 'MS peaks to pathways' tool with significant feature
418 *P*-value cutoff = 0.05. This tool uses mummichog which algorithmically utilizes known metabolic
419 pathways and networks to predict metabolites and pathways without prior identification of
420 metabolites (79). The resulting pathway files from 'perturbed' pairwise feature sets were exported
421 and pathways with less than two significant features (i.e., metabolite features with *P*-values < 0.05)
422 were removed. Next, we filtered the pathways by defining a new parameter, pathway significance
423 factor (psf) (equation 1), to account for i) total number of metabolites in the pathway ($p_{size}$), ii)
424 total identified metabolite features ($p_{features}$), and iii) total number of significant metabolite features
425 ($p_{significant}$) identified for each pathway.

426 $$psf = \frac{1}{psf_{max}} \times \frac{p_{features}}{p_{size}} \times p_{significant}^{0.5} \quad (1)$$

427 In our analysis, we chose a psf cutoff value of 0.58 to illustrate the top 15% most significantly
428 perturbed pathways identified from our untargeted LCMS analysis.

*Targeted LCMS analysis.* Lipidomics raw data files created by Xcalibur were converted to open source mzML format using the ProteoWizard software (80). MAVEN software (Princeton University) was applied to performed retention time correction for each sample and used to manually select known lipids based on retention time and mass (81, 82). Glycerophospholipid headgroup species were analyzed individually and extracted signal intensities were corrected by cell optical density. The corrected intensities for each head group class were summed to visualize changes for each glycerophospholipid on a macro scale.

*Fatty acid quantification.* Three biological replicates of wildtype and YlCW001 cells were grown in 0% and 8% (v/v) [EMIM][OAc] until mid-late exponential phase and cell pellets were stored at -20°C. The equivalent cell mass of 2 $OD_{600nm}$ was washed once with 0.05 M sodium phosphate solution and incubated in 2:1 (v/v) chloroform:methanol solution overnight at 4°C. 200 µL of chloroform was extracted and mild methanolysis was performed as previously described (83). Briefly, 1.5 mL of methanol, 0.3 mL of 8% methanolic HCL solution and 50 µL of 2 mg/mL pentadecanoic acid was added to ensure complete transesterification and incubated overnight at 55°C. After cooling to room temperature, 1mL of hexane containing 0.005 mg/mL pentadecanoic acid ethyl ester as internal standard and 1mL of water was added prior to extracting 250 µL of hexane for GCMS detection of fatty acid methyl esters.

*Sterol quantification.* Three biological replicates of wildtype and YlCW001 cells were grown in 0% and 8% (v/v) [EMIM][OAc] until mid-late exponential phase and cell pellets were stored at -20°C. Sterol quantification was performed with the equivalent cell mass of 5 $OD_{600nm}$ as previously described (84) using a HP-5MS 30 m x 0.25 mm i.d. x 0.25 µm column (Agilent Technologies, USA) for separation of sterols.

*Chitin determination.* The relative quantity of chitin was analyzed for the wildtype and YlCW001 late-exponentially growing cells in medium containing 0%, 2%, 5%, 8% and 10% (v/v) [EMIM][OAc]. Cell pellets were washed twice with water before resuspending 1 $OD_{600nm}$ of cell mass in 1 mL of water containing 50 µg/mL calcofluor white (CFW) (cat #18909, Sigma-Aldrich), which binds specifically to chitin (85, 86). Samples were incubated at room temperature for 15 minutes at 650 rpms in a thermomixer (cat #5382000023, Eppendorf). Next, stained cells were washed twice with water to remove excess CFW prior to fluorescence (excitation: 360/40nm, emission: 460/40nm) and absorbance ($OD_{600nm}$) measurements. Results were calculated by normalizing fluorescence intensity by respective sample OD values. Chitin determination experiments were conducted at least twice for each biological condition in technical replicates per experiment (wildtype 0%, n = 18; wildtype 2%, n = 6; wildtype 5%, n = 15; wildtype 8%, n = 12; YlCW001 0%, n = 25; YlCW001 2%, n = 6; YlCW001 5%, n = 15; YlCW001 8%, n = 29; YlCW001 10%, n = 6).

*Scanning electron microscope (SEM).* Wildtype and YlCW001 cells were inoculated at 1 $OD_{600nm}$ in 0%, and 18% [EMIM][OAc] and 0.3M and 0.6M [BMIM][OAc] in 6-well microtiter plates using an incubating microplate shaker at 28°C and 350 rpm. After 24 hours, cells were collected, immediately washed once with water and incubated in 2% glutaraldehyde containing 10 mM sodium phosphate buffer overnight at 4°C. Fixed samples were washed 3 times with water before post-fixing in 2% osmium tetroxide for 1 hour at room temperature. The cell pellets were placed on silicon chips and dehydrated with successive ethanol baths (50%, 60%, 70%, 80%, 90%, 100%) for 15 minutes each. Finally, the dehydrated samples were dried using critical point drying in carbon dioxide at 1100 psi and 32°C before SEM imaging with Zeiss Argula using SEM2 detector.

*RNA-sequencing of steroid biosynthesis pathway.* In order to investigate response of sterol biosynthesis genes in response to IL, we quantified expression level of the 14 steroid genes annotated in the KEGG database (87) using RNA-sequencing. Three biological replicates of wildtype and YlCW001 were harvested at the mid-exponential growth phase from 0% and 8% (v/v) [EMIM][OAc] and immediately quenched in liquid nitrogen before storing samples at -80°C. Total RNA was purified using a Qiagen RNeasy mini kit (Cat no. 74104, Qiagen Inc, CA, USA). Filtered RNA-sequencing reads were imported and analyzed within the CLC genomics workbench version 11.0.1 (https://www.qiagenbioinformatics.com/) which was also used to calculate differential expression of steroid biosynthesis genes against the wildtype in 0% IL.

*Fluconazole treatment to investigate importance of sterol biosynthesis for enhanced IL tolerance.* To investigate correlation of sterol biosynthesis with enhancement of IL tolerance, we compared growth of the wildtype and YlCW001 in media containing 0% or 8% (v/v) [EMIM][OAc] and various concentrations of fluconazole (cat# TCF0677, VWR) which inhibits fungal cytochrome P450 enzyme 14α-demethylase (Ster4, Fig. 5A) required for sterol biosynthesis (58). First, we cultured the wildtype and YlCW001 in media without IL until the mid-exponential phase. Then, cells were washed by water and resuspended in the fresh media containing 0, 10, 25, 50, 100, and 250 µg/mL fluconazole. Finally, the same conditions were tested with addition of 8% (v/v) [EMIM][OAc] to observe the requirement of sterol incorporation into the plasma membrane for IL tolerance. Results were obtained by calculating maximum specific growth rates for each biological condition. Sterol validation by fluconazole treatment experiments were conducted twice for each biological condition with sacrificial, technical replicates using 96-well microtiter plates and Duetz sandwich cover (cat # SMCR1296, Kuhner) incubated at 28°C and 400 rpms.

*Statistics.* Statistical analysis was performed with SigmaPlot v.14 software using one-way analysis of variance (ANOVA) with Holm-Sidak correction or Student's t-test between biologically relevant conditions where noted.

## Acknowledgement

This research is funded by the National Science Foundation (NSF CBET#1511881). We would like to thank Dr. Stephen Dearth (Biological and Small Molecule Mass Spectrometry Core, UTK) for assistance in metabolomics and lipidomics experiments, Dr. John Dunlap (Advanced Microscopy Imaging Center, UTK) for assistance in SEM experiments, and Mr. Piet Jones (Bredesen Center, UTK) for technical support. The RNAseq work conducted by the U.S. Department of Energy Joint Genome Institute, a DOE Office of Science User Facility, is supported by the Office of Science of the U.S. Department of Energy under Contract No. DE-AC02-05CH11231.

# References

1. Ling H, Teo W, Chen B, Leong SSJ, & Chang MW (2014) Microbial tolerance engineering toward biochemical production: from lignocellulose to products. *Current Opinion in Biotechnology* 29:99-106.

2. Gong Z, Nielsen J, & Zhou YJ (2017) Engineering Robustness of Microbial Cell Factories. *Biotechnology Journal* 12(10):1700014.

3. Nicolaou SA, Gaida SM, & Papoutsakis ET (2010) A comparative view of metabolite and substrate stress and tolerance in microbial bioprocessing: From biofuels and chemicals, to biocatalysis and bioremediation. *Metabolic Engineering* 12(4):307-331.

4. Bokinsky G, *et al.* (2011) Synthesis of three advanced biofuels from ionic liquid-pretreated switchgrass using engineered *Escherichia coli*. *Proceedings of the National Academy of Sciences* 108(50):19949-19954.

5. Park JI, *et al.* (2012) A Thermophilic Ionic Liquid-Tolerant Cellulase Cocktail for the Production of Cellulosic Biofuels. *PLOS ONE* 7(5):e37010.

6. Chen H, *et al.* (2017) A review on the pretreatment of lignocellulose for high-value chemicals. *Fuel Processing Technology* 160:196-206.

7. Ryu S, Labbé N, & Trinh CT (2015) Simultaneous saccharification and fermentation of cellulose in ionic liquid for efficient production of α-ketoglutaric acid by *Yarrowia lipolytica*. *Applied Microbiology and Biotechnology* 99(10):4237-4244.

8. van Rantwijk F & Sheldon RA (2007) Biocatalysis in Ionic Liquids. *Chemical Reviews* 107(6):2757-2785.

9. Yoo CG, Pu Y, & Ragauskas AJ (2017) Ionic liquids: Promising green solvents for lignocellulosic biomass utilization. *Current Opinion in Green and Sustainable Chemistry* 5:5-11.

10. Li C, *et al.* (2010) Comparison of dilute acid and ionic liquid pretreatment of switchgrass: Biomass recalcitrance, delignification and enzymatic saccharification. *Bioresource Technology* 101(13):4900-4906.

11. Mora-Pale M, Meli L, Doherty TV, Linhardt RJ, & Dordick JS (2011) Room temperature ionic liquids as emerging solvents for the pretreatment of lignocellulosic biomass. *Biotechnology and Bioengineering* 108(6):1229-1245.

12. Tadesse H & Luque R (2011) Advances on biomass pretreatment using ionic liquids: An overview. *Energy & Environmental Science* 4(10):3913-3929.

13. Socha AM, *et al.* (2014) Efficient biomass pretreatment using ionic liquids derived from lignin and hemicellulose. *Proc Natl Acad Sci U S A* 111(35):E3587-3595.

14. Cull SG, Holbrey JD, Vargas-Mora V, Seddon KR, & Lye GJ (2000) Room-temperature ionic liquids as replacements for organic solvents in multiphase bioprocess operations. *Biotechnology and Bioengineering* 69(2):227-233.

15. Passos H, Freire MG, & Coutinho JAP (2014) Ionic liquid solutions as extractive solvents for value-added compounds from biomass. *Green chemistry : an international journal and green chemistry resource : GC* 16(12):4786-4815.

16. Sendovski M, Nir N, & Fishman A (2010) Bioproduction of 2-Phenylethanol in a Biphasic Ionic Liquid Aqueous System. *Journal of Agricultural and Food Chemistry* 58(4):2260-2265.

553 17. Ventura SPM, *et al.* (2017) Ionic-Liquid-Mediated Extraction and Separation Processes for
554 Bioactive Compounds: Past, Present, and Future Trends. *Chemical Reviews* 117(10):6984-
555 7052.
556 18. Bauer G, Lima S, Chenevard J, Sugnaux M, & Fischer F (2017) Biodiesel via in Situ Wet
557 Microalgae Biotransformation: Zwitter-Type Ionic Liquid Supported Extraction and
558 Transesterification. *ACS Sustainable Chemistry & Engineering* 5(2):1931-1937.
559 19. Wu Y-W, *et al.* (2016) Ionic Liquids Impact the Bioenergy Feedstock-Degrading
560 Microbiome and Transcription of Enzymes Relevant to Polysaccharide Hydrolysis.
561 *mSystems* 1(6).
562 20. Sitepu IR, *et al.* (2014) Yeast tolerance to the ionic liquid 1-ethyl-3-methylimidazolium
563 acetate. *FEMS Yeast Research* 14(8):1286-1294.
564 21. Yu M, *et al.* (2009) Effects of the 1-alkyl-3-methylimidazolium bromide ionic liquids on
565 the antioxidant defense system of *Daphnia magna*. *Ecotoxicology and environmental*
566 *safety* 72(6):1798-1804.
567 22. Docherty KM & Kulpa JCF (2005) Toxicity and antimicrobial activity of imidazolium and
568 pyridinium ionic liquids. *Green Chemistry* 7(4):185-189.
569 23. Liu L-P, *et al.* (2016) Mechanistic insights into the effect of imidazolium ionic liquid on
570 lipid production by *Geotrichum fermentans*. *Biotechnology for Biofuels* 9(1):266.
571 24. Konda NM, *et al.* (2014) Understanding cost drivers and economic potential of two variants
572 of ionic liquid pretreatment for cellulosic biofuel production. *Biotechnology for Biofuels*
573 7:86-86.
574 25. Lee S-M, Chang W-J, Choi A-R, & Koo Y-M (2005) Influence of ionic liquids on the
575 growth ofEscherichia coli. *Korean Journal of Chemical Engineering* 22(5):687-690.

576 26. Ouellet M, *et al.* (2011) Impact of ionic liquid pretreated plant biomass on *Saccharomyces*
577 *cerevisiae* growth and biofuel production. *Green Chemistry* 13(10):2743-2749.
578 27. Frederix M, *et al.* (2016) Development of an *E. coli* strain for one-pot biofuel production
579 from ionic liquid pretreated cellulose and switchgrass. *Green Chemistry* 18(15):4189-
580 4197.
581 28. Khudyakov JI, *et al.* (2012) Global transcriptome response to ionic liquid by a tropical rain
582 forest soil bacterium, *Enterobacter lignolyticus*. *Proceedings of the National Academy of*
583 *Sciences of the United States of America* 109(32):E2173-E2182.
584 29. Ruegg TL, *et al.* (2014) An auto-inducible mechanism for ionic liquid resistance in
585 microbial biofuel production. *Nature communications* 5:3490.
586 30. Mohamed ET, *et al.* (2017) Generation of a platform strain for ionic liquid tolerance using
587 adaptive laboratory evolution. *Microbial Cell Factories* 16(1):204.
588 31. Dickinson Q, *et al.* (2016) Mechanism of imidazolium ionic liquids toxicity in
589 *Saccharomyces cerevisiae* and rational engineering of a tolerant, xylose-fermenting strain.
590 *Microbial Cell Factories* 15(1):1-13.
591 32. Blazeck J, *et al.* (2014) Harnessing *Yarrowia lipolytica* lipogenesis to create a platform for
592 lipid and biofuel production. *Nature communications* 5:3131.
593 33. Xu P, Qiao K, Ahn WS, & Stephanopoulos G (2016) Engineering *Yarrowia lipolytica* as a
594 platform for synthesis of drop-in transportation fuels and oleochemicals. *Proceedings of*
595 *the National Academy of Sciences* 113(39):10848-10853.
596 34. Sitepu I, Selby T, Lin T, Zhu S, & Boundy-Mills K (2014) Carbon source utilization and
597 inhibitor tolerance of 45 oleaginous yeast species. *Journal of Industrial Microbiology &*
598 *Biotechnology* 41(7):1061-1070.

599 35. N Andreishcheva E, *et al.* (1999) *Adaptation to Salt Stress in a Salt-Tolerant Strain of the*
600 *Yeast Yarrowia lipolytica* pp 1061-1067.
601 36. Biryukova EN, Medentsev AG, Arinbasarova AY, & Akimenko VK (2006) Tolerance of
602 the yeast *Yarrowia lipolytica* to oxidative stress. *Microbiology* 75(3):243-247.
603 37. Yu C, Simmons BA, Singer SW, Thelen MP, & VanderGheynst JS (2016) Ionic liquid-
604 tolerant microorganisms and microbial communities for lignocellulose conversion to
605 bioproducts. *Applied Microbiology and Biotechnology*:1-13.
606 38. da Costa Lopes AM, João KG, Morais ARC, Bogel-Łukasik E, & Bogel-Łukasik R (2013)
607 Ionic liquids as a tool for lignocellulosic biomass fractionation. *Sustainable Chemical*
608 *Processes* 1(1):1.
609 39. Heckenbach ME, Romero FN, Green MD, & Halden RU (2016) Meta-analysis of ionic
610 liquid literature and toxicology. *Chemosphere* 150:266-274.
611 40. Liu H, Zhang X, Chen C, Du S, & Dong Y (2015) Effects of imidazolium chloride ionic
612 liquids and their toxicity to *Scenedesmus obliquus*. *Ecotoxicology and environmental*
613 *safety* 122:83-90.
614 41. Lim GS, Jaenicke S, & Klahn M (2015) How the spontaneous insertion of amphiphilic
615 imidazolium-based cations changes biological membranes: a molecular simulation study.
616 *Physical chemistry chemical physics : PCCP* 17(43):29171-29183.
617 42. Mehmood N, *et al.* (2018) *Kluyveromyces marxianus*, an Attractive Yeast for Ethanolic
618 Fermentation in the Presence of Imidazolium Ionic Liquids. *International Journal of*
619 *Molecular Sciences* 19(3):887.

620 43. Lindberg L, Santos AXS, Riezman H, Olsson L, & Bettiga M (2013) Lipidomic Profiling
621 of *Saccharomyces cerevisiae* and *Zygosaccharomyces bailii* Reveals Critical Changes in
622 Lipid Composition in Response to Acetic Acid Stress. *PLOS ONE* 8(9):e73936.
623 44. Santos AXS & Riezman H (2012) Yeast as a model system for studying lipid homeostasis
624 and function. *FEBS Letters* 586(18):2858-2867.
625 45. Lipke PN & Ovalle R (1998) Cell Wall Architecture in Yeast: New Structure and New
626 Challenges. *Journal of Bacteriology* 180(15):3735-3740.
627 46. Ingram LO (1976) Adaptation of membrane lipids to alcohols. *Journal of Bacteriology*
628 125(2):670-678.
629 47. Santos AG, Ribeiro BD, Alviano DS, & Coelho MAZ (2014) Toxicity of ionic liquids
630 toward microorganisms interesting to the food industry. *RSC Advances* 4(70):37157-
631 37163.
632 48. Yoo B, Shah JK, Zhu Y, & Maginn EJ (2014) Amphiphilic interactions of ionic liquids
633 with lipid biomembranes: a molecular simulation study. *Soft Matter* 10(43):8641-8651.
634 49. Lee H (2015) Effects of imidazolium-based ionic surfactants on the size and dynamics of
635 phosphatidylcholine bilayers with saturated and unsaturated chains. *Journal of Molecular*
636 *Graphics and Modelling* 60:162-168.
637 50. Yoo B, Zhu Y, & Maginn EJ (2016) Molecular Mechanism of Ionic-Liquid-Induced
638 Membrane Disruption: Morphological Changes to Bilayers, Multilayers, and Vesicles.
639 *Langmuir* 32(21):5403-5411.
640 51. Wu Y, Sasaki T, Irie S, & Sakurai K (2008) A novel biomass-ionic liquid platform for the
641 utilization of native chitin. *Polymer* 49(9):2321-2327.

642 52. Lesage G & Bussey H (2006) Cell Wall Assembly in *Saccharomyces cerevisiae*.
643 *Microbiology and Molecular Biology Reviews* 70(2):317-343.
644 53. Ishmayana S, Kennedy UJ, & Learmonth RP (2017) Further investigation of relationships
645 between membrane fluidity and ethanol tolerance in *Saccharomyces cerevisiae*. *World*
646 *Journal of Microbiology and Biotechnology* 33(12):218.
647 54. Tan Z, Yoon JM, Nielsen DR, Shanks JV, & Jarboe LR (2016) Membrane engineering via
648 trans unsaturated fatty acids production improves *Escherichia coli* robustness and
649 production of biorenewables. *Metabolic Engineering* 35:105-113.
650 55. Kohlwein SD (2017) Analyzing and Understanding Lipids of Yeast: A Challenging
651 Endeavor. *Cold Spring Harbor Protocols* 2017(5):pdb.top078956.
652 56. Caspeta L, *et al.* (2014) Altered sterol composition renders yeast thermotolerant. *Science*
653 346(6205):75-78.
654 57. Vanegas Juan M, Contreras Maria F, Faller R, & Longo Marjorie L (2012) Role of
655 Unsaturated Lipid and Ergosterol in Ethanol Tolerance of Model Yeast Biomembranes.
656 *Biophysical Journal* 102(3):507-516.
657 58. de Souza W & Rodrigues JCF (2009) Sterol Biosynthesis Pathway as Target for Anti-
658 trypanosomatid Drugs. *Interdisciplinary Perspectives on Infectious Diseases* 2009:19.
659 59. Fan L-L, Li H-J, & Chen Q-H (2014) Applications and Mechanisms of Ionic Liquids in
660 Whole-Cell Biotransformation. *International Journal of Molecular Sciences* 15(7):12196-
661 12216.
662 60. Mehmood N, *et al.* (2015) Impact of two ionic liquids, 1-ethyl-3-methylimidazolium
663 acetate and 1-ethyl-3-methylimidazolium methylphosphonate, on *Saccharomyces*

*cerevisiae*: metabolic, physiologic, and morphological investigations. *Biotechnol Biofuels* 8.

61. Galluzzi M, *et al.* (2013) Interaction of Imidazolium-Based Room-Temperature Ionic Liquids with DOPC Phospholipid Monolayers: Electrochemical Study. *Langmuir* 29(22):6573-6581.

62. Yoo B, *et al.* (2016) Molecular mechanisms of ionic liquid cytotoxicity probed by an integrated experimental and computational approach. *Scientific Reports* 6:19889.

63. Stock F, *et al.* (2004) Effects of ionic liquids on the acetylcholinesterase - a structure-activity relationship consideration. *Green Chemistry* 6(6):286-290.

64. Auxenfans T, Husson E, & Sarazin C (2017) Simultaneous pretreatment and enzymatic saccharification of (ligno) celluloses in aqueous-ionic liquid media: A compromise. *Biochemical Engineering Journal* 117:77-86.

65. Nargotra P, Vaid S, & Bajaj B (2016) Cellulase Production from *Bacillus subtilis* SV1 and Its Application Potential for Saccharification of Ionic Liquid Pretreated Pine Needle Biomass under One Pot Consolidated Bioprocess. *Fermentation* 2(4):19.

66. Sandoval NR & Papoutsakis ET (2016) Engineering membrane and cell-wall programs for tolerance to toxic chemicals: beyond solo genes. *Current opinion in microbiology* 33:56-66.

67. Tan Z, *et al.* (2017) Engineering *Escherichia coli* membrane phospholipid head distribution improves tolerance and production of biorenewables. *Metabolic Engineering* 44:1-12.

68. de Kroon AIPM, Rijken PJ, & De Smet CH (2013) Checks and balances in membrane phospholipid class and acyl chain homeostasis, the yeast perspective. *Progress in lipid research* 52(4):374-394.

687 69. Renne MF & de Kroon AIPM (2018) The role of phospholipid molecular species in
688 determining the physical properties of yeast membranes. *FEBS Letters* 592(8):1330-1345.
689 70. Yang Z, *et al.* (2017) Fluconazole inhibits the cellular ergosterol synthesis to confer
690 synergism to berberine against yeast cells. *Journal of Global Antimicrobial Resistance*.
691 71. Cromie SRT, Del Pópolo MG, & Ballone P (2009) Interaction of Room Temperature Ionic
692 Liquid Solutions with a Cholesterol Bilayer. *The Journal of Physical Chemistry B*
693 113(34):11642-11648.
694 72. Russo G, Witos J, Rantamäki AH, & Wiedmer SK (2017) Cholesterol affects the
695 interaction between an ionic liquid and phospholipid vesicles. A study by differential
696 scanning calorimetry and nanoplasmonic sensing. *Biochimica et Biophysica Acta (BBA) -*
697 *Biomembranes* 1859(12):2361-2372.
698 73. Klahn M & Zacharias M (2013) Transformations in plasma membranes of cancerous cells
699 and resulting consequences for cation insertion studied with molecular dynamics. *Physical*
700 *chemistry chemical physics : PCCP* 15(34):14427-14441.
701 74. Rabinowitz JD & Kimball E (2007) Acidic Acetonitrile for Cellular Metabolome
702 Extraction from *Escherichia coli*. *Analytical Chemistry* 79(16):6167-6173.
703 75. Lu W, *et al.* (2010) Metabolomic Analysis via Reversed-Phase Ion-Pairing Liquid
704 Chromatography Coupled to a Stand Alone Orbitrap Mass Spectrometer. *Analytical*
705 *Chemistry* 82(8):3212-3221.
706 76. Cassilly CD, *et al.* (2017) Role of phosphatidylserine synthase in shaping the
707 phospholipidome of *Candida albicans*. *FEMS Yeast Research* 17(2):fox007-fox007.

77. Tautenhahn R, Patti GJ, Rinehart D, & Siuzdak G (2012) XCMS Online: A Web-Based Platform to Process Untargeted Metabolomic Data. *Analytical Chemistry* 84(11):5035-5039.

78. Xia J & Wishart DS (2016) Using MetaboAnalyst 3.0 for Comprehensive Metabolomics Data Analysis. *Current Protocols in Bioinformatics* 55(1):14.10.11-14.10.91.

79. Li S, *et al.* (2013) Predicting Network Activity from High Throughput Metabolomics. *PLOS Computational Biology* 9(7):e1003123.

80. Martens L, *et al.* (2011) mzML—a Community Standard for Mass Spectrometry Data. *Molecular & Cellular Proteomics : MCP* 10(1):R110.000133.

81. Melamud E, Vastag L, & Rabinowitz JD (2010) Metabolomic Analysis and Visualization Engine for LC−MS Data. *Analytical Chemistry* 82(23):9818-9826.

82. Clasquin MF, Melamud E, & Rabinowitz JD (2002) LC-MS Data Processing with MAVEN: A Metabolomic Analysis and Visualization Engine. *Current Protocols in Bioinformatics*, (John Wiley & Sons, Inc.).

83. Ichihara Ki & Fukubayashi Y (2010) Preparation of fatty acid methyl esters for gas-liquid chromatography. *Journal of Lipid Research* 51(3):635-640.

84. Santivañez-Veliz M, *et al.* (2017) Development, validation and application of a GC–MS method for the simultaneous detection and quantification of neutral lipid species in *Trypanosoma cruzi*. *Journal of Chromatography B* 1061-1062:225-232.

85. Richard M, Quijano RR, Bezzate S, Bordon-Pallier F, & Gaillardin C (2001) Tagging Morphogenetic Genes by Insertional Mutagenesis in the Yeast *Yarrowia lipolytica*. *Journal of Bacteriology* 183(10):3098-3107.

730 86. Sheng W, Yamashita S, Ohta A, & Horiuchi H (2013) Functional Differentiation of Chitin
731 Synthases in *Yarrowia lipolytica*. *Bioscience, Biotechnology, and Biochemistry*
732 77(6):1275-1281.
733 87. Kanehisa M, Sato Y, Kawashima M, Furumichi M, & Tanabe M (2016) KEGG as a
734 reference resource for gene and protein annotation. *Nucleic Acids Research* 44(D1):D457-
735 D462.

736

## Figure legends

**Fig 1.** Evolutionary engineering of IL-tolerant *Y. lipolytica* strains. **Step 1**: Adaptive laboratory evolution of *Y. lipolytica* on various concentrations of [EMIM][OAc]. **Step 2**: Single mutant isolation on plates without IL. **Step 3**: Mutant characterization to elucidate the underlying mechanism of solvent tolerance. `

**Fig 2. (A)** Adaptive laboratory evolution of *Y. lipolytica* grown with increasing concentrations of [EMIM][OAc]. **(B, C)** Irreversibility testing of the evolved *Y. lipolytica* strain YlCW001 in various concentrations of [EMIM][OAc]. **(D, E)** Broad tolerance test for growth of *Y. lipolytica* wildtype and mutant at various concentrations of 0.6M and 1.09M ILs. Error bars represent the standard deviation of three independent biological replicates repeated twice (n=6). Abbreviations: [EMIM][OAc]: 1-ethyl-3-methylimidizolium acetate; [EMIM][Cl]: 1-ethyl-3-methylimidizolium chloride; [EMIM][Br]: 1-ethyl-3-methylimidizolium bromide acetate; [BMIM][OAc]: 1-butyl-3-methylimidazolium; [BMIM][Cl]: 1-butyl-3-methylimidizollium chloride; [BMIM][Br]: 1-butyl-3-methylimidazolium bromide; and [AMIM][Cl]: 1-allyl-3-methylimidizolium chloride.

**Fig. 3**. SEM imaging of the wildtype and YlCW001 cells exposed to **(A, B)** no IL, **(C, D)** 18% (v/v) [EMIM][OAc], **(E, F)** 0.3M [BMIM][OAc], and **(G, H)** 0.6M [BMIM][OAc]. **(I)** IL-responsive pathways perturbed with respect to wildtype *Y. lipolytica* growing in medium without IL with a psf score > 0.58. Biological triplicates were performed for all biological conditions and results were combined from hydrophilic metabolomics extraction (negative ionization, n = 3), and hydrophobic lipidomics extractions (negative ionization, n = 3; positive ionization, n = 3).

**Fig. 4**. Glycerophospholipid and fatty acid reorganization in wildtype *Y. lipolytica* and YlCW001 in 0% and 8% (v/v) [EMIM][OAc]. (**A**) PC: Phosphatidylcholine (F = 11.038) (**B**) PI: phosphatidylinositol (F = 14.147); (**C**) PA: phosphatidic acid (F = 31.234); (**D**) PG: phosphatidyl glycerol (F = 29.562); (**E**) PS: phosphatidylserine (degree of freedom = 1; wildtype 8%, F = 19.953; YlCW001 0%, F = 104.891; YlCW001 8%, F = 3.097); (**F**) PE: phosphatidylethanolamine (F = 26.321); (**G**) CL: cardiolipin (F = 8.157). (**H**) Fatty acid distributions (C16:1, F = 9.501; C16:0, F = 4.768; C18:2, F = 13.4; C18:1, F = 84.261; C18:0, F = 2.839). (**I**) Chemical structures of glycerophospholipid backbone and headgroup species. All error bars represent standard deviation of biological triplicates (n=3) and statistical significance was calculated using one-way analysis of variance (ANOVA) with Holm-Sidak correction against control group, wildtype in 0% IL (degrees of freedom, 3). Symbols: "*": $p$-value < 0.05; "**": $p$-value < 0.01; "***", $p$-values < 0.001.

**Fig. 5.** (**A**) Steroid biosynthesis pathway in *Y. lipolytica*. Fluconazole is an antifungal drug that inhibits sterol 14-demethylase (Ster4) (**B**) Differential gene expression of the steroid pathway as compared to the wildtype strain in medium without IL (Ster1, YALI0A10076g; Ster2, YALI0E15730g; Ster3, YALI0F04378g; Ster4, YALI0B05126g; Ster5, YALI0B23298g; Ster6, YALI0F11297g; Ster7, YALI0C22165g; Ster8, YALI0B17644g; Ster9, YALI0F08701g; Ster10-1, YALI0E32065g; Ster10-2, YALI0B17204g; Ster11, YALI0D20878g; Ster12, YALI0A18062g; Ster13, YALI0D19206g). (**C**) Effect of fluconazole inhibiting the steroid pathway on cell growth. Error bars represent standard deviation from three technical replicates repeated twice per biological condition (n = 6) (**D**) Relative ergosterol content of wildtype and YlCW001 strains in

783 0% and 8% (v/v) [EMIM][OAc]. Error bars represent standard deviation of biological triplicates
784 (n =3) and statistical significance was calculated between the wildtype and YlCW001 in 8% IL
785 using the Student's t-test (t = -4.244 with 4 degrees of freedom). Abbreviation: "**", *p*-value =
786 0.013.
787
788 **Fig. 6.** Mechanisms of IL interference and tolerance in wildtype *Y. lipolytica* and YlCW001. (**A,**
789 **D**) No IL exposure. (**B, E**) IL exposure and interference. (**C, D**) Cellular membrane response.
790

**Fig. 1**

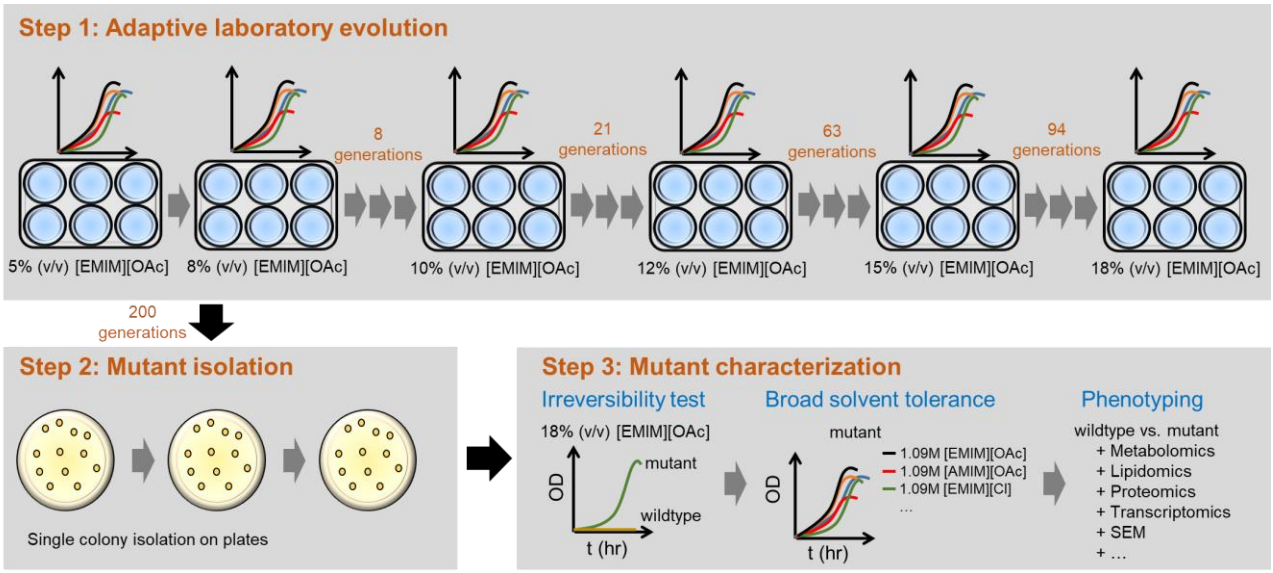

801 **Fig. 2**

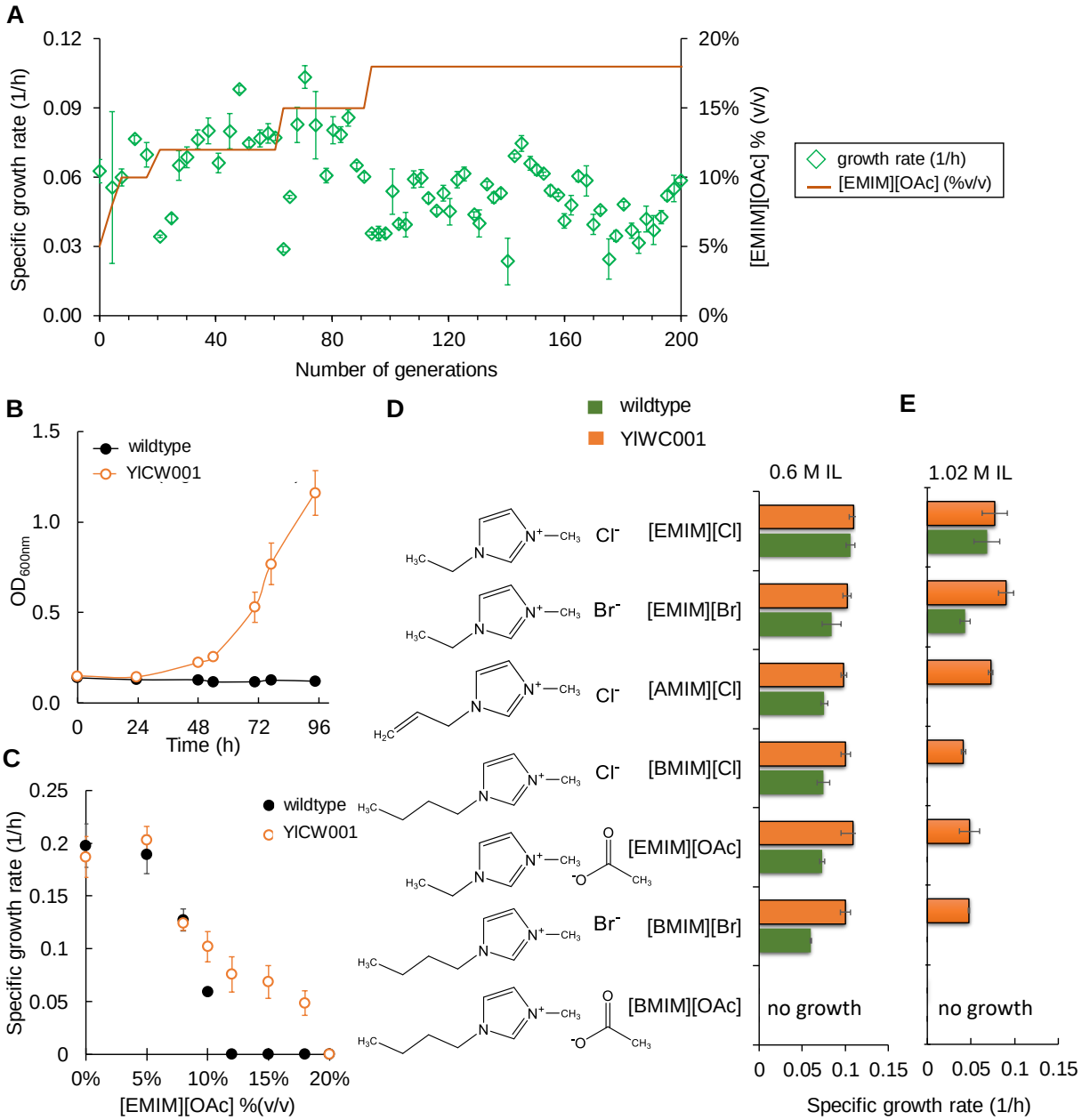


802

803

804 **Fig. 3**

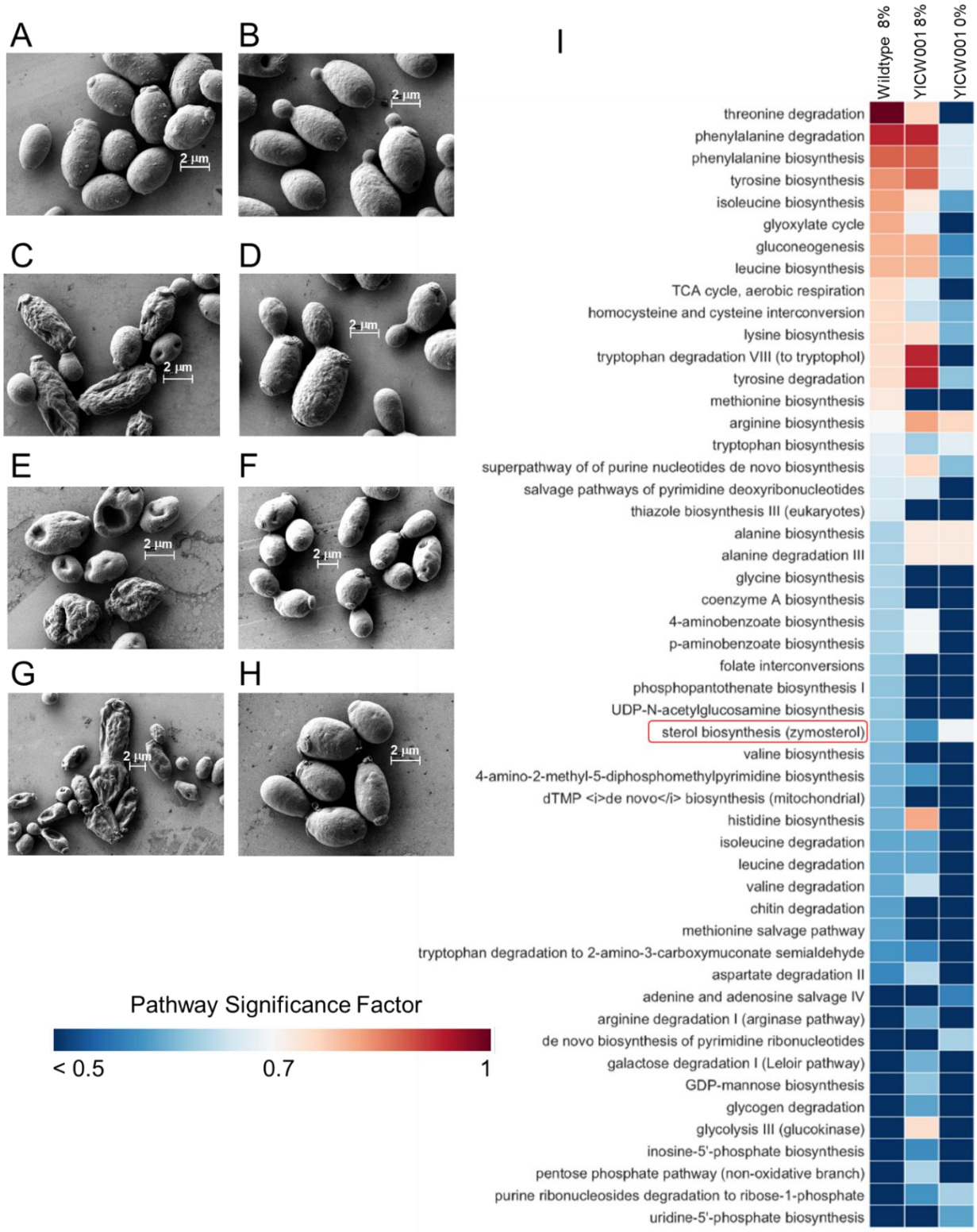


805

806

807 **Fig. 4**

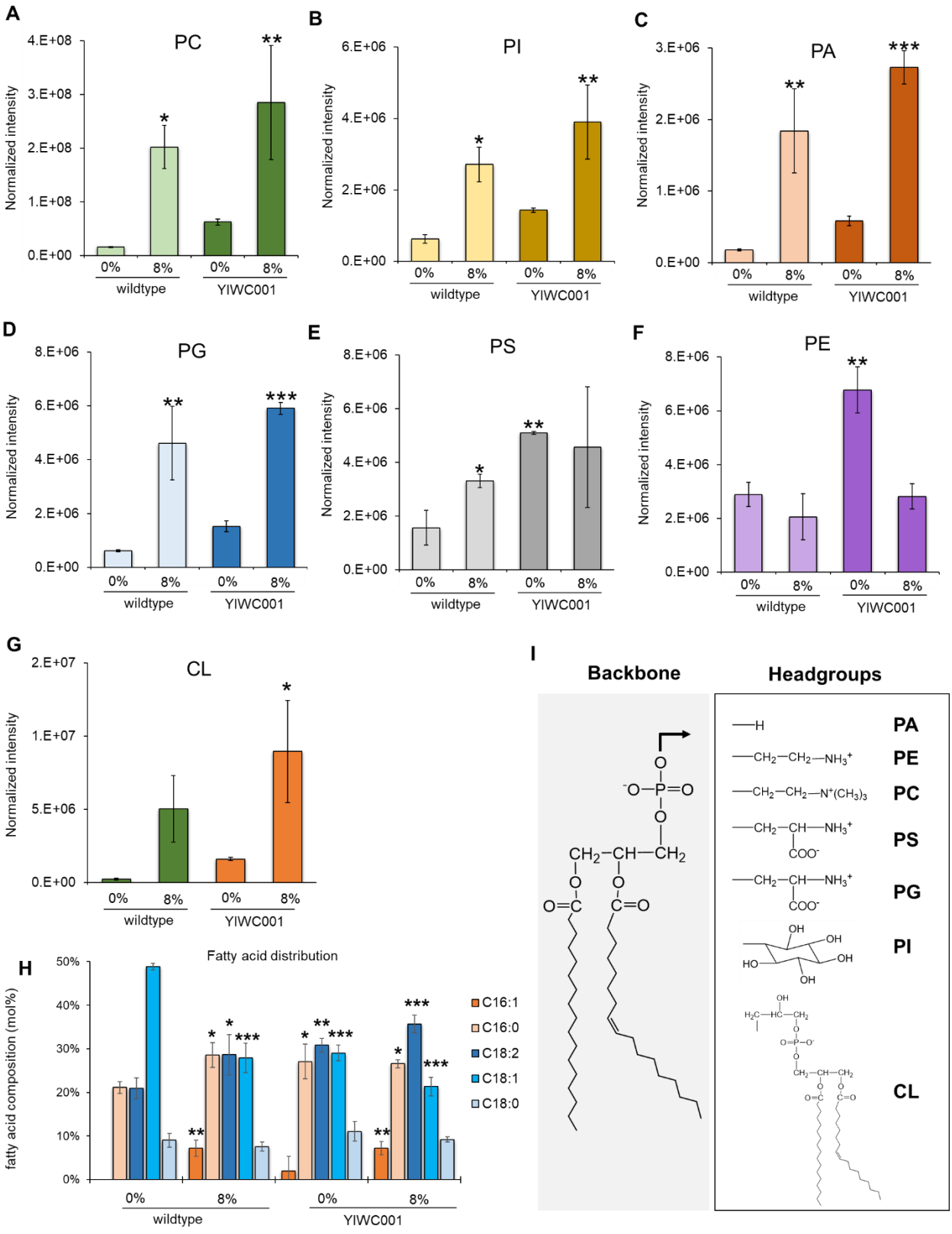


808

809 **Fig. 5**

810

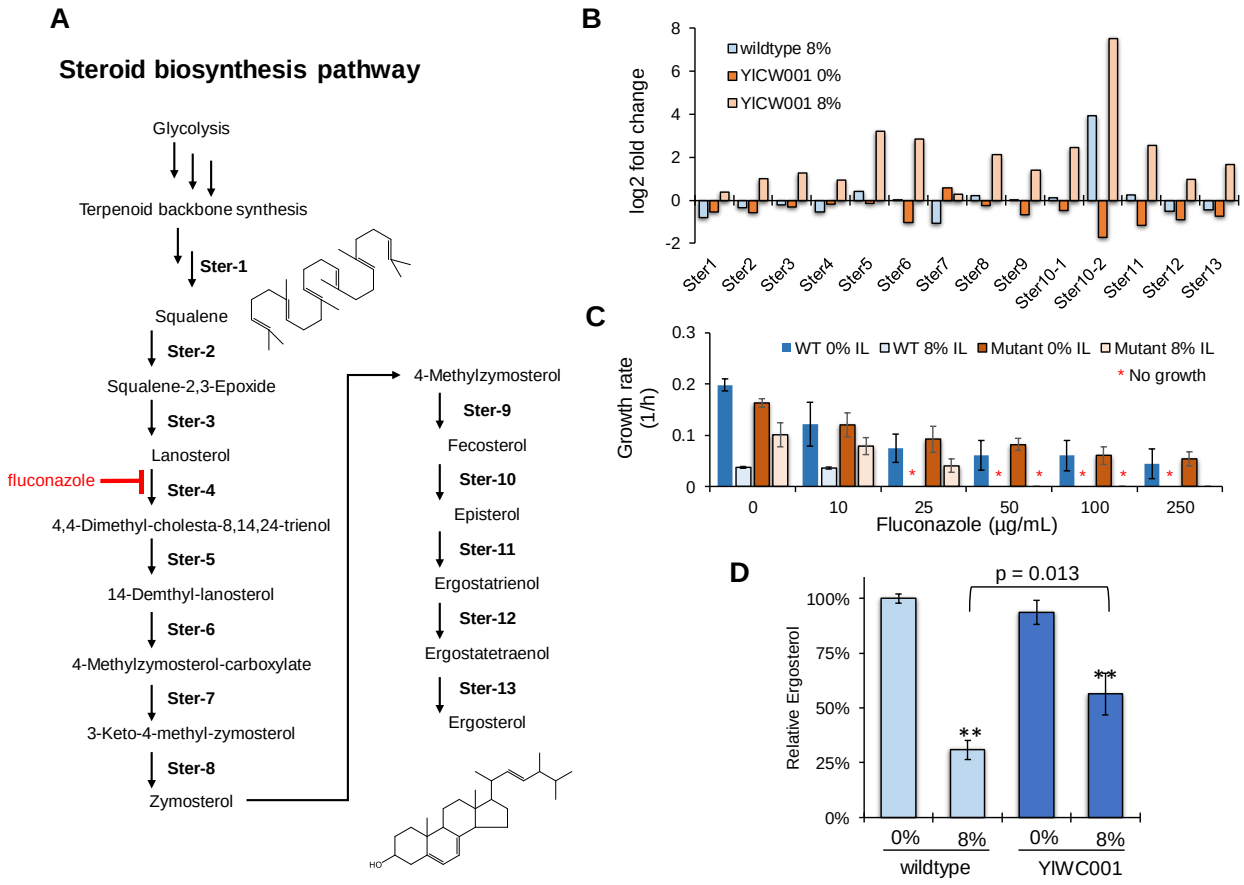


811

812

813 **Fig. 6**

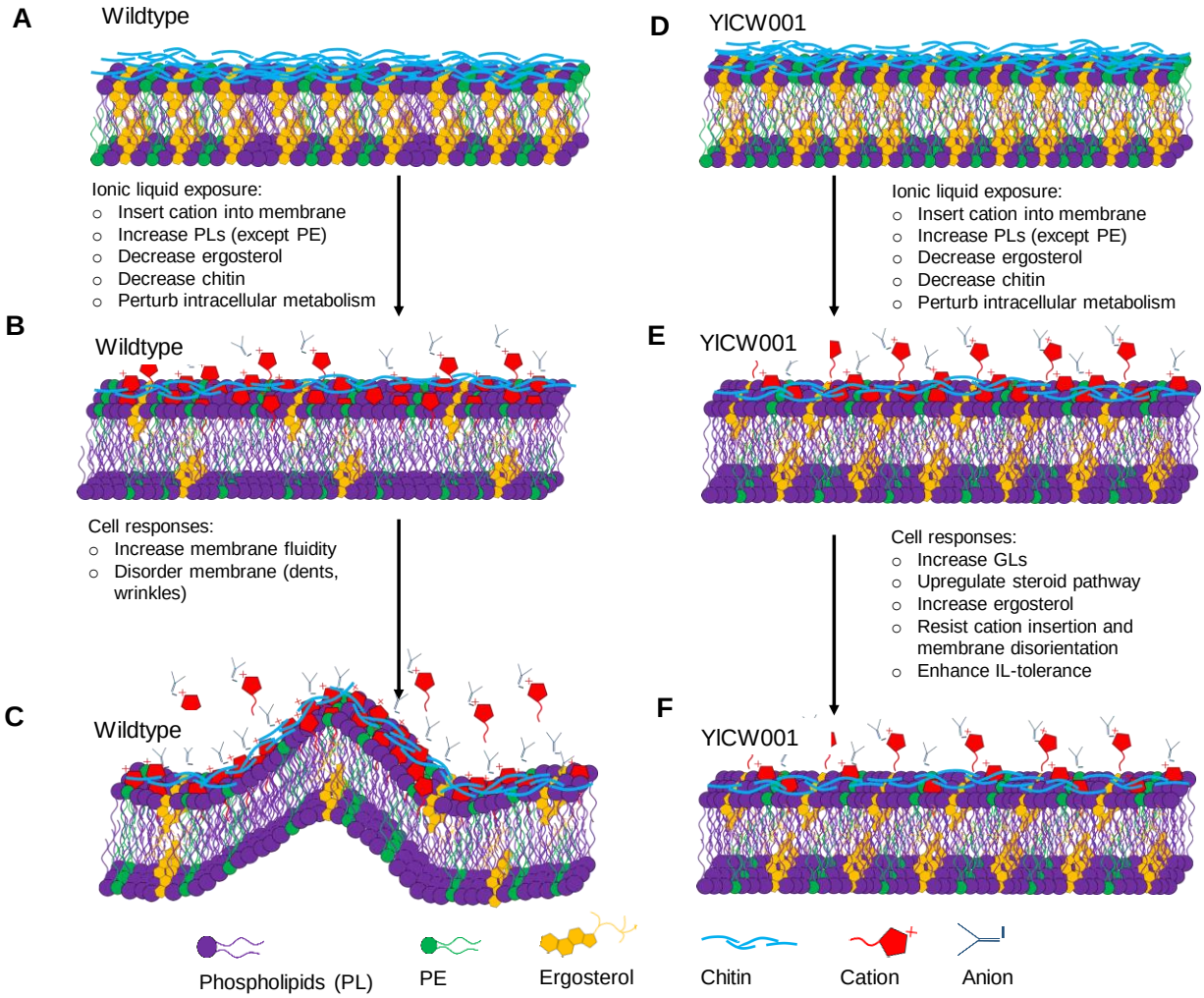


814

815